

## TIMING THE GEMINGA PULSAR WITH GAMMA-RAY OBSERVATIONS

J. R. MATTOX

Astronomy Department, Boston University, 725 Commonwealth Avenue, Boston, MA 02215; Mattox@bu.edu

J. P. HALPERN

Department of Astronomy, Columbia University, 550 West 120th Street, New York, NY 10027;  
jules@carmen.phys.columbia.edu

AND

P. A. CARAVEO

Istituto di Fisica Cosmica del CNR, via Bassini, 15, 20133 Milano, Italy; pat@eros.ifctr.mi.cnr.it

Received 1997 April 28; accepted 1997 September 10

### ABSTRACT

We present the *COS B*/EGRET 1997 ephemeris for the rotation of the Geminga pulsar. This ephemeris is derived from high-energy  $\gamma$ -ray observations that span 24 yr. The recently obtained accurate position and proper motion are assumed. A cubic ephemeris predicts the rotational phase of Geminga with errors smaller than 50 milliperiods for all existing high-energy  $\gamma$ -ray observations that span a 24.2 yr timing baseline. The braking index obtained is  $17 \pm 1$ . Further observation is required to ascertain whether this high value truly reflects the rotational energy loss mechanism, or whether it is a manifestation of timing noise. The ephemeris parameters are sufficiently constrained so that timing noise will be the limitation on forward extrapolation. If Geminga continues to rotate without a glitch, as it has for at least 23 yr, we expect this ephemeris to continue to describe the phase, with an error of less than 100 milliperiods, until 2008. Statistically significant timing residuals are detected in the EGRET data that depart from the cubic ephemeris at a level of 30 milliperiods. Although this could simply be an additional manifestation of timing noise, the EGRET timing residuals appear to have a sinusoidal modulation that is consistent with a planet of mass  $1.7/\sin i M_{\oplus}$  orbiting Geminga at a radius of 3.3 AU.

*Subject headings:* gamma rays: observations — pulsars: individual (Geminga)

### 1. INTRODUCTION

The isolated pulsar Geminga is the second brightest Galactic high-energy  $\gamma$ -ray source in the sky (Thompson et al. 1977; Bennett et al. 1977; Bertsch et al. 1992), but it is not detected in the radio, except perhaps weakly at 100 MHz (Kuzmin & Losovsky 1997; Malofeev & Malov 1997; Shitov & Pugachev 1997; Vats et al. 1997). Therefore, high-energy observations are currently the principal means of timing the rotation of Geminga. The *ROSAT* detection of periodic X-ray emission (Halpern & Holt 1992) with a period of 237 ms led to a successful search for periodicity in the nearly contemporaneous EGRET data (Bertsch et al. 1992), as well as in the archival *COS B* (Bignami & Caraveo 1992; Hermsen et al. 1992) and *SAS 2* data (Mattox et al. 1992). This established the fact that Geminga is a rotation-powered pulsar with a surface magnetic field  $B_p \sim 1.6 \times 10^{12}$  G and a spin-down age  $\tau = P/2\dot{P} = 3.4 \times 10^5$  yr. Preliminary analyses of the EGRET data were presented by Mayer-Hasselwander et al. (1994) and Fierro et al. (1997). For a recent review of Geminga, see Bignami & Caraveo (1996). *ASCA* and *Extreme-Ultraviolet Explorer (EUVE)* results were presented by Halpern, Martin, & Marshall (1996) and Halpern & Wang (1997). Caraveo et al. (1996) reported the detection with the *Hubble Space Telescope (HST)* of a parallactic displacement of the optical counterpart of  $0''.0064 \pm 0''.0017$ , which implies a distance of  $157^{+59}_{-34}$  pc. Caraveo et al. (1997) also obtained a position for the optical counterpart of Geminga that is accurate to  $\sim 40$  mas by using the *Hipparcos* data to locate accurately field stars in the *HST* Geminga exposure.

Although the periodicity of Geminga was initially found

in *ROSAT* X-ray data, much more precise timing can be done with EGRET, because the *ROSAT* exposures are short, the soft-X-ray peaks are broad, and their modulation is shallow. An ephemeris for the rotation of Geminga based on EGRET observations spanning 2.1 yr was published by Mattox et al. (1994). Subsequently, an ephemeris for observations spanning 3.9 yr was published (Mattox, Halpern, & Caraveo 1996). With this 3.9 yr timing baseline, Mattox et al. (1996) found a significant sharpening of the light curve when the proper motion was used, as is expected if the optical object is the source of the  $\gamma$ -ray emission. New observations have now extended the baseline of EGRET observations to 5.9 yr. This long baseline allows the rotation parameters of Geminga to be sufficiently constrained, so that the rotation phase during EGRET observations can be compared to the phase during *COS B* observations. We thus obtain a cubic ephemeris that describes the rotation of Geminga from the beginning of *SAS 2* observations (1973.0) to the end of the most recent EGRET observation (1997.2), with timing residuals that are less than 50 milliperiods. With the second derivative of frequency tightly constrained by this long baseline, significant timing residuals have become apparent.

### 2. DERIVATION OF A CUBIC EPHEMERIS FROM THE *SAS 2*, *COS B*, AND EGRET OBSERVATIONS

As described by Mattox et al. (1994, 1996), the ephemeris parameters are estimated as the values that give the largest value of the  $Z_{10}^2$  statistic (i.e., the most nonuniform light curve). We seek a simple representation of the time dependence of the phase of Geminga. The first three terms of a

Taylor series form a cubic ephemeris:

$$\phi = \phi_0 + f(t - t_0) + \dot{f}(t - t_0)^2/2 + \ddot{f}(t - t_0)^3/6, \quad (1)$$

where  $t_0$  is the epoch, and  $t$  is time at the solar system barycenter. Error in the position used when correcting photon arrival times to the barycenter can cause error in the derived ephemeris parameters (e.g., Bisnovatyi-Kogan & Postnov 1993). Mattox et al. (1996) show that the maximum possible error in corrected arrival time is  $2.3\delta_e$  ms, where  $\delta_e$  is the position error in arcseconds. With the ability to resolve the phase to  $\sim 5$  milliperiods with  $\gamma$ -ray observations to date, errors in the position of Geminga of larger than  $0.5$  will affect the timing solution. The recent determination of the time-dependent position of Geminga to within  $\sim 40$  mas (Caraveo et al. 1997) is an order of magnitude better than is required for this timing analysis. The position at the epoch of an *HST* observation and the proper motion given in Table 1 are used for our analysis.

In order to compare the rotational phase of Geminga during the *COS B* observations to the EGRET phase, we have updated the *COS B* barycenter vector. This was required because the MIT PEP 740 ephemeris for the solar system used by the *COS B* team yields a barycenter position that is at a substantial distance from the barycenter position obtained with the JPL DE 200 solar system ephemeris used by the EGRET team. This discrepancy results from updated values for the masses of the outer planets, obtained recently through spacecraft flyby. The update for the *COS B* data was not simple, because the position of the *COS B* spacecraft for each event is not available in modern databases. Rather than attempting to resurrect and reanalyze a large number of old magnetic tapes, we have used the MIT PEP 740 ephemeris to recover the *COS B* spacecraft position from the old barycenter direction vector for each *COS B* event. These positions were observed to be consistent with the *COS B* orbit. The spacecraft position for each *COS B* event was then used with the JPL planetary ephemeris to obtain a new barycenter direction vector for each event. The resulting change in the barycenter arrival times for *COS B* Geminga events ranged between 6.3 and 10.1 ms. The *SAS 2* data included the spacecraft position for each event, allowing the JPL DE 200 ephemeris to be used directly.

We initially analyzed the EGRET data alone. With the new observations (concluding on 1997 March 18), the EGRET observations now span 5.9 yr. We previously analyzed EGRET events that were selected for energy  $E > 70$  MeV (Mattox et al. 1994, 1996). However, an investigation of the potential for resolving rotation phase with EGRET data, described below, led to a new energy selection for this work of  $E > 100$  MeV. No resulting loss in timing accuracy is observed. In addition, variation in the shape of the light curve with the spectral response of EGRET as the spark-chamber gas ages, and the consequent impact on phase measurement, is reduced with this selection. Events were selected from an energy-dependent cone encompassing 68% of the PSF at each energy. To eliminate contamination from Earth albedo  $\gamma$ -rays, the minimum accepted angle from the horizon was an energy-dependent  $3\sigma$  cut, based on the EGRET PSF.

The downhill simplex method (Press et al. 1992) was used to estimate simultaneously the  $f$  and  $\dot{f}$  that produced a maximum  $Z_{10}^2$  statistic for various  $\dot{f}$ . This search only finds local maxima. Previous grid searches (as described by Mattox et al. 1994, 1996) allowed us to begin the downhill

simplex search near a timing solution that lines up phase for each observation—as confirmed through epoch-folding each exposure separately.

The cubic ephemeris thus obtained for EGRET with  $T_0 = \text{JD } 2448750.5$  is  $f = 4.21766909394(3)$ ,  $\dot{f} = -1.95226(1) \times 10^{-13}$ , and  $\ddot{f} = 8.0(8) \times 10^{-25}$ . The uncertainty of the last digit of each parameter is indicated by the digit in parentheses. This corresponds to a decrease by 5.1 in the  $Z_{10}^2$  statistic, corresponding to a bootstrap determination of the 95% confidence interval (Mattox et al. 1994). A full analysis of covariance has not been done. However, in determining the uncertainty of  $\dot{f}$ , both  $f$  and  $\ddot{f}$  were optimized for each value of  $\dot{f}$  considered. Likewise, in determining the uncertainty of  $\ddot{f}$ ,  $f$  was optimized for each value of  $\dot{f}$  considered. The corresponding braking index,  $\eta = \dot{f}/f^2 = 89 \pm 9$ , is much higher than the value of  $\eta = 3$  expected for magnetic dipole radiation. This discrepancy is discussed below.

The same analysis was done for the *COS B* data alone. See Mattox et al. (1992) for the *COS B* light curve. With  $T_0 = \text{JD } 2443946.5$ , the cubic ephemeris is  $f = 4.2177501227(1)$ ,  $\dot{f} = -1.95239(2) \times 10^{-13}$ , and  $\ddot{f} = 4.5(2.0) \times 10^{-25}$ . This implies a braking index  $\eta = 50 \pm 20$  that is consistent with that of Hermsen et al. (1992). Because the accurate position and proper motion of Caraveo et al. (1997) were used for this analysis, we can reject the hypothesis of Bisnovatyi-Kogan & Postnov (1993) that the large value of  $\dot{f}$  that was reported by Hermsen et al. (1992) is caused by proper motion. Another explanation is proposed in §4.

We note that the *COS B* and EGRET values for  $\dot{f}$  are inconsistent. Furthermore, the value obtained from the two measurements of  $\dot{f}$ ,

$$\dot{f} = \frac{\dot{f}_{\text{EGR}} - \dot{f}_{\text{COS}}}{T_{0\text{EGR}} - T_{0\text{COS}}} = 3.1(5) \times 10^{-26}, \quad (2)$$

although consistent with a braking index of 3, is not consistent with either the *COS B* value for  $\dot{f}$  or with the EGRET value. These discrepancies can be attributed to timing noise. However, they make the search for a timing solution that would coherently connect *COS B* and EGRET problematic. Nonetheless, having coherent solutions for 6.7 yr of *COS B* data and 5.9 yr of EGRET data, it seemed plausible that one could find a coherent solution that would bridge the 9.0 yr between these observations.

In the search for a coherent *COS B*/EGRET timing solution, the downhill simplex method was used to estimate  $f$ ,  $\dot{f}$ , and  $\ddot{f}$ . An epoch near the center of the *COS B*/EGRET timespan was chosen. The search was initiated at  $\sim 1000$  different initial values of these three parameters in order to attempt to find a global maximum in the midst of hundreds of local maxima. After several days of processing, a solution was found that gave a value of  $Z_{10}^2 = 3283$  that was distinctly larger than the rest. The next best value was 3043. The cubic ephemeris thus obtained for *COS B*/EGRET with  $T_0 = \text{JD}2446600$  is

$$\begin{aligned} f &= 4.217705363090(13), \\ \dot{f} &= -1.9521717(12) \times 10^{-13}, \\ \ddot{f} &= 1.48(3) \times 10^{-25}. \end{aligned} \quad (3)$$

The uncertainty of the last digit of each parameter (95% confidence—corresponding to a decrease by 5.1 in the  $Z_{10}^2$

TABLE 1  
*COS B*/EGRET 1997 EPHEMERIS FOR GEMINGA OBTAINED THROUGH A COHERENT ANALYSIS OF *SAS 2*,  
*COS B*, AND EGRET DATA

Parameter	Value
Epoch $T_0$ (JD) .....	2446600 (1986 June 18.5 Barycentric Dynamical Time)
Frequency at epoch $f$ (Hz) .....	4.217705363081(13)
Frequency derivative $\dot{f}$ (Hz s <sup>-1</sup> ) .....	$-1.9521712(12) \times 10^{-13}$
2nd frequency derivative $\ddot{f}$ (Hz s <sup>-2</sup> ) .....	$1.49(3) \times 10^{-25}$
Position $\alpha_{2000}, \delta_{2000}$ at JD 2449794 .....	6 <sup>h</sup> 33 <sup>m</sup> 54 <sup>s</sup> .153, +17° 46' 12".91
Proper motion at position angle 54° (mas yr <sup>-1</sup> ) .....	169; $\mu_{\alpha_{2000}} = 138, \mu_{\delta_{2000}} = 97$
Possible Binary Term	
Projected semimajor axis $a_1 \sin i$ (lt-ms) .....	6.2(9)
Orbital period $P_b$ (yr) .....	5.1(1)
Epoch of periastron passage $T_b$ .....	JD 2449360(20)
Longitude of periastron $\omega$ .....	90°
Eccentricity $e$ .....	0.0(4)
Assuming $M_1 = 1.4 M_\odot$	
$a_2$ (AU) .....	3.31(4)
$M_2 \sin i$ ( $M_\oplus$ ) .....	1.7(2)

NOTE.—Digit in parentheses following the derived parameters is the ~95% confidence uncertainty of the last digit. See Fig. 1 legend for a definition of peak 1. Peak 1 occurs 0.556(2) of a rotation after  $T_0$

statistic) is indicated by the digit in parentheses. The light curve obtained with equation (2) for the EGRET data is shown in Figure 1.

Equation (2) produces a light curve for each observation that was found, through visual inspection, to be consistent with an invariant shape and phase, after allowing for variable instrument response and statistical fluctuation. The local maxima have parameters that are clearly distinct from equation (2), and the phase of the  $\gamma$ -ray peaks were observed to be discrepant between observations, if events were epoch-folded with the parameters of any of the local maxima. We also find that the 81 *SAS 2* Geminga events ( $E > 100$  MeV; Mattox et al. 1992) yield a phase that is consistent with *COS B* and EGRET when epoch-folded with equation (2). Equation (2) is therefore thought to be an accurate description of the rotation of Geminga from the time of the *SAS 2*

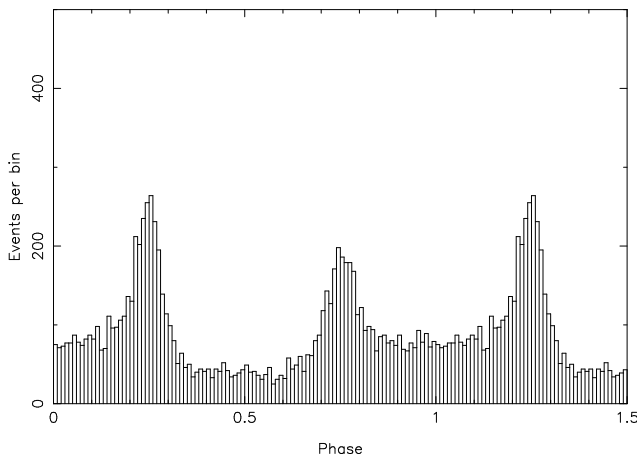


FIG. 1.—Phase dependence of the Geminga  $\gamma$ -rays detected by EGRET with  $E > 100$  MeV as obtained with the ephemeris of eq. (3). A phase offset of 0.194 has been added for the purpose of display, so that peak 1 is at phase 0.75. Peak 1 precedes the strongest emission bridge, the “major bridge” interval. The “minor bridge” interval follows peak 2. The histograms contain 8877 events from EGRET observations between 1991.3 and 1997.2. The event selection is described in the text.

observations through the EGRET observations. Because of this long timing interval, the parameters of this cubic ephemeris are much more precisely determined than for previous Geminga ephemerides.

The braking index implied by equation (2) is  $17 \pm 1$ . We discuss in § 4 the discrepancy with the value of 3 that is expected if magnetic dipole radiation is the dominant energy loss mechanism. A detailed analysis of the timing residuals follows.

It is of interest to compare the uncertainties of the parameters in equation (2) with expectation. A rough estimate of the expected resolution of each term in a cubic ephemeris is

$$\delta f \approx \frac{q}{\Delta T} = 1.5 \times 10^{-11} \text{ Hz}, \quad (4)$$

$$\delta \dot{f} \approx \frac{2q}{\Delta T^2} = 4 \times 10^{-20} \text{ Hz s}^{-1}, \quad (5)$$

$$\delta \ddot{f} \approx \frac{6q}{\Delta T^3} = 2 \times 10^{-28} \text{ Hz s}^{-2}, \quad (6)$$

where  $q$  is the typical phase resolution of a  $\gamma$ -ray observation,  $q \sim 0.01$ , and  $\Delta T$  is the 21.6 yr from the first *COS B* exposure to the last EGRET exposure. The resolution found for  $f$  in equation (2) slightly exceeds this expectation. The resolution of  $\dot{f}$  in practice is a factor of 3 worse, and the resolution of  $\ddot{f}$  a factor of 15 worse. This reflects the fact that the higher order terms in a Taylor series cause increasing phase variation far from the epoch, and the resolution is therefore worse because phase must be determined with a small fraction of the exposure. As expected, the discrepancy is more pronounced for the cubic term than for the quadratic term.

We note, in passing, that the transverse velocity of Geminga  $v_t = 122 \text{ km s}^{-1}$  causes the observed  $\dot{f}$  to be larger than the intrinsic value  $\dot{f}_i$  by the kinematic contribution  $\dot{f}_k = f_i v_t^2 / cD$  (Shklovskii 1970), where  $D$  is the distance. For Geminga, this is not an important effect ( $\dot{f}_k / \dot{f}_i = 2 \times 10^{-4}$ ), because  $\dot{f}_i$  is relatively large.

### 3. ANALYSIS OF GAMMA-RAY TIMING RESIDUALS

With abundant Geminga events from a deep EGRET exposure, a visual inspection of the light curve can resolve phase to  $\sim 10$  milliperiods. However, with the very sparse statistics of *SAS 2*, *COS B*, and weak EGRET exposures, it is not feasible to assess phase accurately through a visual inspection. Therefore, a means of quantitatively assessing  $\gamma$ -ray phase has been developed.

This analysis is made more difficult by the dramatic changes of the spectrum of the  $\gamma$ -ray emission of Geminga with phase (Mayer-Hasselwander et al. 1994; Fierro et al. 1997). The different spectral responses and background levels of the three  $\gamma$ -ray telescopes thus result in different light curves. Also, the spectral response of each telescope becomes gradually harder as the spark-chamber gas ages, then reverts to a softer response when the gas is replaced. Since a detailed model of the dynamic spectrum is not available (R. Romani 1997, private communication), an empirical approach has been taken.

The light curve of each Geminga observation was fitted with the following ad hoc function:

$$\begin{aligned}
 F(\phi) &= F_{b_2} + (F_{p_2} - F_{b_2})[1 + (\phi - \phi_2)^2/W_{p_{2a}}^2]^{-1} \\
 &\quad \phi_2 - 0.25 < \phi < \phi_2 \\
 F(\phi) &= F_{b_1} + (F_{p_2} - F_{b_1})[1 + (\phi - \phi_2)^2/W_{p_{2b}}^2]^{-1} \\
 &\quad + (F_{p_1} - F_{b_1})[1 + (\phi - \phi_1)^2/W_{p_{1a}}^2]^{-1} \\
 &\quad \phi_2 < \phi < \phi_1, \\
 F(\phi) &= F_{b_2} + (F_{p_1} - F_{b_2})[1 + (\phi - \phi_1)^2/W_{p_{1b}}^2]^{-1} \\
 &\quad \phi_1 < \phi < \phi_1 + 0.25. \quad (7)
 \end{aligned}$$

This equation has four Lorentzian functions, one for each side of each peak. The phase of peak 1 is fixed relative to peak 2,  $\phi_1 = \phi_2 + 0.500$ , as discussed below. The peak widths are fixed at values obtained from a deep EGRET exposure that provide 39 days of exposure in a 54 day interval (1991 April 22–June 15; henceforth designated as VP 0.2–2.5):  $W_{p_{2a}} = 0.0297$ ,  $W_{p_{2b}} = 0.0233$ ,  $W_{p_{1a}} = 0.0343$ , and  $W_{p_{1b}} = 0.0287$ . Five parameters were adjusted using the downhill simplex algorithm to optimize the fit to each observation:  $\phi_2$ , the phase of peak 2;  $F_{b_2}$ , the flux level of the major bridge;  $F_{b_1}$ , the flux level of the minor bridge;  $F_{p_2}$ , the flux level of peak 2; and  $F_{p_1}$ , the flux level of peak 1. A phase ambiguity of  $180^\circ$  is averted because  $F_{b_2} > F_{b_1}$ .

The fit was compared to binned events, and the quality of the fit was assessed by a calculation of the  $\chi^2$  statistic for the difference. The width of each phase bin was adjusted to obtain a specific number of observed events in each bin. Ten events per bin were found to work well, even for weak exposures. Larger numbers of events per bin worked as well for strong exposures. The values of  $\chi^2$  obtained were generally smaller than the number of bins minus the number of optimized parameters, indicating that equation (7) is a satisfactory representation of the light curve, and that variation in spectral response and background is accommodated. Figure 2 shows this fit in comparison to histograms of EGRET events. Because five parameters are fitted, the uncertainty of the phase estimate is demarcated by the change in  $\phi_2$  that causes an increase in  $\chi^2$  of 5.9 for 68% confidence.

Initial work with the deep EGRET exposure obtained in VP 0.2–2.5 found that the the separation of the two peaks is

in fact  $500 \pm 5$  milliperiods. Each peak was analyzed using data in a phase interval of  $\sim 0.5$ , centered on the peak. An analysis of the hardness ratio of Geminga as a function of phase (Fierro et al. 1997) finds that the hardening of each peak is approximately symmetric about the peak. Thus, we can expect that our method of finding the phase of a peak is not strongly affected by differences in the spectral responses of the instruments. In fact, an analysis by this method of the all EGRET exposure through 1996.7 found that the phases of both peaks 1 and 2 are invariant for the energy bands  $150 < E < 500$  MeV and  $500 < E < 30,000$  MeV. However, the peaks in the  $70 < E < 150$  MeV energy band were both shifted by 10 milliperiods toward smaller phase. Thus, an energy selection of  $E > 100$  MeV was adopted for this work. Other than the expected variation of  $F_{b_-}$  and  $F_{p_-}$  with instrument spectral response, no indication of time variability in the light curve was seen.

Equation (7) was used to obtain a value for the timing residual for each observation of Geminga after epoch-folding with the cubic ephemeris in equation (3). The resulting residuals are shown in Figure 3a. Some of the EGRET viewing periods have been combined for this analysis, either to provide adequate statistics, or because they are close in time. The VP 0.2–2.5 exposures have thus been combined. These exposures were also analyzed separately, and they gave consistent phase. Because timing noise that is large enough to detect is not expected on this time-scale, the latter provides reassurance that our timing residual analysis is correct.

The fact that these residuals are small can be used to constrain the size of any Geminga glitch during this era. We have concluded that no glitch larger than  $\Delta\nu/\nu < 5 \times 10^{-10}$  has occurred between 1973 and 1996.6, i.e., between the *SAS 2* observation and the penultimate EGRET observation, based on the following considerations. The most likely glitch behavior for an older pulsar (Shemar & Lyne 1996) is a permanent change in rotational frequency. An increase in the rotational frequency of Geminga by  $\Delta\nu = 5 \times 10^{-10}\nu$  after the beginning of EGRET observations, but before 1996.6, would have caused a phase discrepancy of at least 39 milliperiods at the time of the 1997.2 EGRET observation. Similarly, an increase in the rotational frequency of Geminga by  $\Delta\nu = 5 \times 10^{-10}\nu$  immediately following the *SAS 2* observation in 1973 would have caused a phase change of at least 169 milliperiods, relative to the phase observed with *COS B* during the first observation at 1975.5.

Finally, a glitch near the end of the *COS B* observations or between the *COS B* and EGRET observations would prevent us from finding a cubic ephemeris that aligns phase during all five *COS B* observations and all 10 EGRET observations. The validity of this assertion was established with the help of the following computational experiment. We used the  $Z_{10}^2$  statistic to search for a cubic ephemeris that would align phase for all observations, after we added  $\frac{1}{2}$  of the rotation period to all *SAS 2* and *COS B* arrival times. As in the derivation of equation (3), we used the downhill simplex method to optimize  $f$ ,  $\dot{f}$ , and  $\ddot{f}$ , starting from  $\sim 1000$  different initial values of these three parameters. The optimal cubic ephemeris thus found was equivalent to equation (3), i.e., the *SAS 2* and *COS B* phase remained shifted by  $180^\circ$  in the optimal solution for the deformed data. This was immediately apparent upon examination of phase for individual observations. The value of  $Z_{10}^2$  was consequently reduced from 3283 to 3137. This

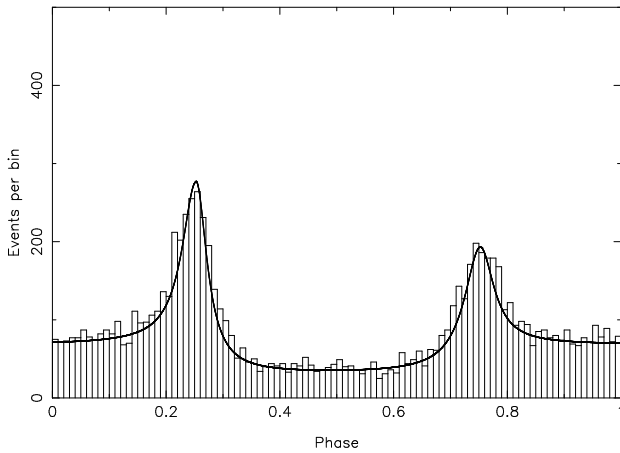


FIG. 2a

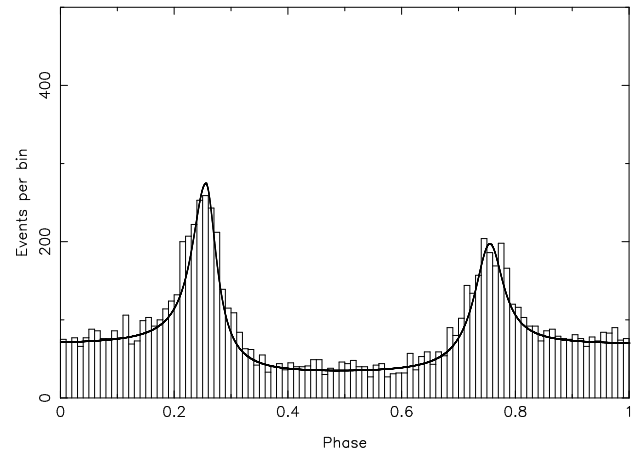


FIG. 2b

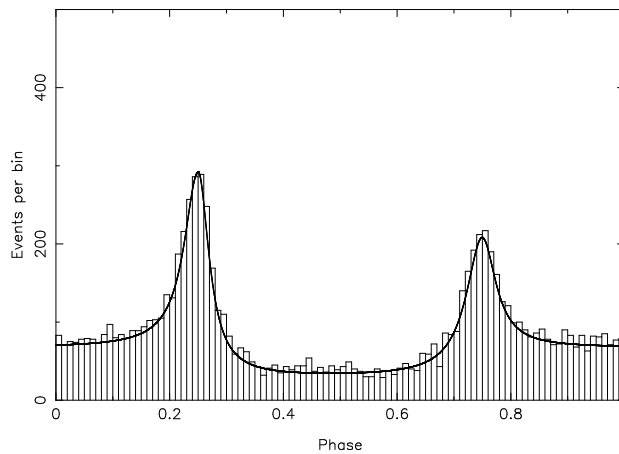


FIG. 2c

FIG. 2.—Fit of eq. (7) for the phase dependence of the Geminga  $\gamma$ -rays is superposed on the histogram of EGRET event phases. Events are selected as in Fig. 1. A phase offset of 0.194 has been added for display. The fit obtained with eq. (7) is shown with a heavy line for each histogram. (a) Events have been epoch-folded with the ephemeris of eq. (3). The optimum value of  $\phi_2$  used in the fit is 0.253. (b) Events have been epoch-folded with the cubic ephemeris of Table 1, only without the sinusoidal term. The optimum value of  $\phi_2$  used in the fit is 0.250. (c) Events have been epoch-folded with the cubic ephemeris of Table 1, including the sinusoidal term. The optimum value of  $\phi_2$  used in the fit is 0.256.

artificial distortion of arrival times is equivalent in effect to that of a  $\Delta v/v = 4 \times 10^{-10}$  glitch occurring just after the last *COS B* observation (with an “antiglitch” just prior to the first EGRET observation to restore a lower rotational

frequency). We thus confirmed our ability to detect a  $\Delta v \approx 5 \times 10^{-10}v$  glitch.

From an examination of the  $f$  and  $\dot{f}$  values of the 14 pulsars that have been observed to glitch (Shemar & Lyne

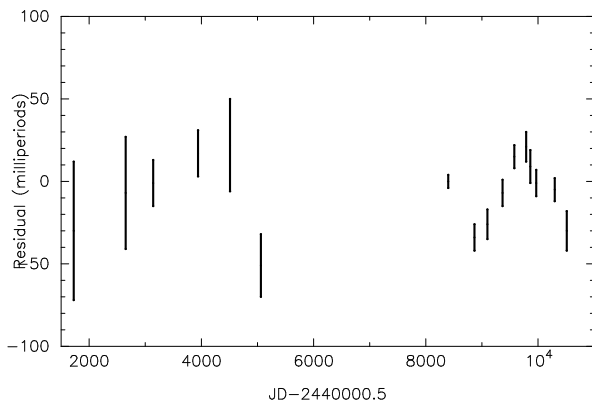


FIG. 3a

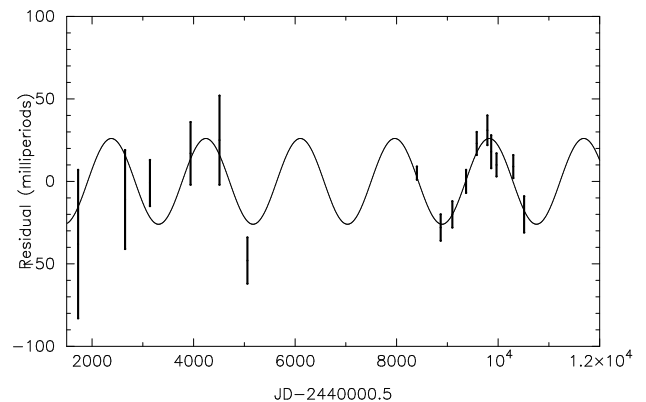


FIG. 3b

FIG. 3.—Timing residuals for Geminga. The error bars demarcate 68% confidence ranges. The first residual at JD 2441725 is from the *SAS 2* observation. The residuals from JD 2442651 to JD 2445061 are from the *COS B* observation. Subsequent residuals are from EGRET observations. (a) Timing residuals for Geminga, relative to the cubic ephemeris of eq. (3), with the phase obtained for VP 0.2–2.5 defining zero. (b) Timing residuals relative to the cubic ephemeris of Table 1, excluding the sinusoidal term. The sinusoidal term in Table 1 is shown with the continuous line.

1996), in comparison with all pulsars (Taylor, Manchester, & Lyne 1993), we find that the absence of a Geminga glitch over  $\sim 23$  yr is not unexpected. This implies that we can count each of the 3.2 billion rotations of Geminga that have occurred during the last 24 yr, including 1.2 billion rotations during the 9 yr interval between *COS B* and EGRET observations.

For the EGRET observations, modulation in the timing residual that is consistent with a sinusoid with a period of  $\sim 5$  yr is apparent in Figure 3. However, with EGRET observations covering only  $\sim 1$  potential period, and with only modest precision in the determination of the values of the timing residuals, it is possible that this is simply timing noise (Cordes 1993). Assuming that these residuals are timing noise, the activity parameter of Geminga can be calculated. For comparison with studies of large numbers of pulsars, values of timing residuals were obtained relative to the optimal quadratic ephemeris for the EGRET data alone ( $T_0 = \text{JD } 2448750.5$ ,  $\dot{f} = 0$ ,  $f = 4.21766909351(3)$ , and  $\ddot{f} = -1.95179(1) \times 10^{-13}$ ). The rms value of the residual is 23 milliperiods, or 5.4 ms. For reference, the Crab pulsar residuals are expected to be 19 ms for a 5.9 yr timing baseline (Cordes 1993). Thus the activity parameter of Geminga is  $\log(5.4/19) = -0.54$ . Examination of Figure 2 of Cordes (1993) indicates that this value is somewhat larger than expected for a pulsar with the period and period derivative of Geminga. Also, if the modulation is timing noise, quasi-sinusoidal modulation is not likely. Examination of Figure 1 of Cordes (1993) indicates that only  $\sim 10\%$  of pulsars exhibit timing noise that could appear as sinusoidal, as our residuals do. Therefore, it is plausible that the apparent sinusoidal modulation is caused by a planet, and the range of acceptable values for the parameters of a binary system have been explored.

The downhill simplex method was used to find the optimal  $f$ ,  $\dot{f}$ , and  $\ddot{f}$  for the combined *SAS 2*, *COS B*, and EGRET data as various orbital parameters were tried. This led to the orbital parameters given in Table 1, along with the corresponding cubic ephemeris. The values of  $f$ ,  $\dot{f}$ , and  $\ddot{f}$  in Table 1 differ from those in equation (2) by less than the  $1\sigma$  uncertainty of each parameter, reflecting the fact that the orbital term is a very minor modification of the timing solution. However, the value of the  $Z_{10}^2$  statistic is increased to 3666 upon epoch-folding with Table 1, compared to  $Z_{10}^2 = 3283$  for equation (2).

An eccentricity of 0.3 yields a further increase of the  $Z_{10}^2$  statistic to 3674. This increase of 8 is not highly significant, so an eccentricity of zero is assumed. The uncertainty of each orbital parameter was obtained by noting the change that caused a decrease by  $\sim 5$  in the  $Z_{10}^2$  statistic (Mattox et al. 1994 found, from a bootstrap analysis, that a decrease by 5.1 in the  $Z_{10}^2$  indicated the 95% confidence interval for  $f$  and  $\dot{f}$ ). The resulting ephemeris is given in Table 1. The timing residuals are shown in Figure 3b. The cubic ephemeris with the sinusoidal term given in Table 1 is an acceptable representation:  $\chi^2 = 13.7$  for 10 degrees of freedom (dof). For the optimal cubic ephemeris (eq. [3]),  $\chi^2 = 54.7$  for 13 dof ( $\chi^2 = 67.3$  for the cubic ephemeris of Table 1 without the planetary term). This indicates, with a significance of  $5 \times 10^{-7}$ , that we have detected timing residuals relative to the optimal cubic ephemeris.

The  $F$ -test, using these values of  $\chi^2$ , indicates with 97% confidence that the cubic ephemeris of Table 1 with the binary term is a significant improvement in the representa-

tion of the data, considering the additional free parameters introduced. The increase of the  $Z_{10}^2$  statistic by 383 indicates the improvement perhaps even more strongly. Comparison of the panels of Figure 2 shows that the EGRET peaks are visibly broader when the binary term is not used. Of course, it is possible that this sinusoidal term is coincidentally a good representation of timing noise over this 6 yr interval. If a planet exists, the rms residual is the deviation from the sinusoidal fit in the bottom panel of Figure 3, 5.6 milliperiods or 1.3 ms. This is about the same as our phase resolution, so it is regarded as an upper limit. The corresponding upper limit on the activity parameter is  $-1.2$ . Examination of Figure 2 of Cordes (1993) indicates that a value of less than  $-1.2$  for Geminga is plausible.

#### 4. DISCUSSION

The absence of annual modulation in Figure 3 demonstrates that the position of Caraveo et al. (1997) is not in error by more than  $\sim 0.5$ . And the fact that the timing residuals obtained with Table 1 (even without the sinusoidal term) are less than 50 milliperiods for all observations strongly suggests that this ephemeris is in fact a coherent solution for the combined *SAS 2*, *COS B*, and EGRET data. It is now clear why the optimal cubic ephemeris for the EGRET data alone implies a braking index of 90. The large second derivative is a partial fit to the timing residuals of Figure 3. The extended timing baseline that *COS B* provides allows a braking index of 90 to be ruled out. We expect that the large second derivative in the *COS B* data alone is also caused by this effect. The braking index of  $17 \pm 1$  implied by the coherent solution probably reflects timing noise as well. But if it is an intrinsic property of Geminga's spin-down, then it may indicate that Geminga's  $\gamma$ -ray luminosity is decreasing very rapidly as it spins down. Perhaps Geminga is approaching its demise at the outer-gap death line (Chen & Ruderman 1993). Continued timing of Geminga is warranted for distinguishing an intrinsic high braking index from timing noise.

If further timing observations establish the reality of the Geminga planet, it would be the second confirmed pulsar planet. Two (and perhaps more) planets are known to orbit millisecond pulsar PSR B1257+12 (Wolszczan 1994). Also, modulation of timing residuals is seen that may indicate planets orbiting PSR B1620-26 (Thorsett, Arzoumanian, & Taylor 1993) and PSR B0329+54 (Shabanova 1995). If confirmed, the Geminga planet would be the first confirmed planet around a "slow" pulsar. Such a planet must either have survived the supernova explosion or have been formed from the ejecta of the supernova, rather than from material accreted from a secondary star, as is possible for a spun-up pulsar, which PSR B1257+12 is suspected to be.

If confirmed, the Geminga planet would be the nearest pulsar planetary system, and as such would be interesting to study in the IR. Assuming an Earth-like planet that is heated by an isotropic wind of particles and  $\gamma$ -rays carrying Geminga's spin-down power of  $3 \times 10^{34}$  ergs  $s^{-1}$ , it would have a luminosity of  $\sim 2 \times 10^{24}$  ergs  $s^{-1}$  and a temperature of  $\sim 260$  K. At a distance of 160 pc, the planet's flux at 10  $\mu\text{m}$  would be  $\sim 1.2$  nJy.

Two sources of emission would compete with the thermal IR flux from the planet. The first is the surface of the neutron star itself, and the second is nonthermal emission from the pulsar magnetosphere. The thermal flux from the pulsar at 10  $\mu$  is expected to be  $\sim 0.2$  nJy. More serious

competition is likely to come from nonthermal emission that might be associated with the excess X-ray and optical flux that is clearly present above the extrapolation of the thermal soft-X-ray component. Geminga has a hard-X-ray power-law component that has been modeled (Wang et al. 1997) as synchrotron emission from  $e^\pm$  pairs of initial energy of  $\sim 100$  MeV that are produced by the conversion of  $\gamma$ -rays on the magnetic field near the surface of the neutron star. In this model, a  $\nu^{-0.5}$  power law between  $\sim 0.1$  and  $\sim 5$  MeV is produced as pairs instantaneously radiate all their energy locally in the magnetic field of  $\sim 10^{10}$  G on closed field lines. Since the local cyclotron energy is  $\sim 0.1$  keV, the synchrotron spectrum must break below this energy to a spectrum that is proportional to  $\nu^{+1/3}$  at low frequencies. Therefore, we hypothesize that Geminga's excess optical emission is this synchrotron tail, and that it extends into the IR as  $\nu^{1/3}$ . Adopting a non-thermal flux of  $0.1 \mu\text{Jy}$  at  $0.5 \mu$ , we estimate a nonthermal contribution of  $\sim 37$  nJy at  $10 \mu$ , which is large, compared to any planetary emission.

### 5. CONCLUSIONS

We have obtained a cubic ephemeris that describes coherently all  $\gamma$ -ray observations of the rotational phase of Geminga. It appears that Geminga has not glitched during the last 23 yr. If Geminga continues to rotate without a glitch, we expect that the ephemeris we present in Table 1 will describe its rotation until 2008, with a phase error of

less than 100 milliperiods. The derived braking index,  $17 \pm 1$ , may be a manifestation of timing noise.

We have developed a new technique for assessing the phase of  $\gamma$ -ray emission. We find that the two peaks in the Geminga high-energy light curve are separated by  $500 \pm 5$  milliperiods. We also find highly significant timing residuals, relative to a cubic ephemeris, that have the appearance of sinusoidal modulation. With the observations available now, it is not possible to distinguish a planet orbiting Geminga with a period of 5.1 yr from timing noise. Given the wide range of potential timing-noise activity for Geminga, neither interpretation implies an unusual activity parameter for the timing noise of Geminga. We expect that EGRET observations could confirm the timing-noise hypothesis in the near future, but that establishing the existence of a planet would take many years, and possibly use high-quality data from the proposed *GLAST* mission (Michelson et al. 1996).

J. M. acknowledges support from NASA grants NAG 5-3384 and NAG 5-3806, and J. H. from NASA grant NAG 5-2051. We thank J. Cordes and J. Lazio for running their genetic algorithm on our timing residuals in search of potential planetary solutions. We thank D. Thompson for comments and for expediting the delivery of EGRET VP 616.1 data. We also thank D. Helfand, J. Cordes, V. Kaspi, and S. Kulkarni for useful discussions, and an anonymous referee for useful suggestions.

### REFERENCES

- Bennett, K., et al. 1977, *A&A* 56, 469  
 Bertsch, D. L., et al. 1992, *Nature*, 357, 306  
 Bignami, G. F., & Caraveo, P. A. 1992, *Nature*, 357, 287  
 ———, 1996, *ARA&A*, 34, 331  
 Bisnovatyi-Kogan, G. S., & Postnov, K. A. 1993, *Nature*, 366, 663  
 Caraveo, P. A., Bignami, G. F., Mignani, R., & Taff, L. G. 1996, *ApJ*, 461, L91  
 Caraveo, P. A., Lattanzi, M. G., Massone, G., Mignani, R., Makarov, V. V., Perryman, M. A. C., & Bignami, G. F. 1997, *A&A, Lett.*, in press  
 Chen, K., & Ruderman, M. 1993, *ApJ*, 402, 264  
 Cordes, J. M. 1993, in *ASP Conf. Ser.* 36, *Planets around Pulsars*, ed. J. Phillips, S. Thorsett, & S. Kulkarni (San Francisco: ASP), 43  
 Fierro, J. M., Michelson, P. F., Nolan, P. L., & Thompson, D. J. 1998, *ApJ*, 494, in press  
 Halpern, J. P., & Holt, S. S. 1992, *Nature*, 357, 222  
 Halpern, J. P., Martin, C., & Marshall, H. L. 1996, *ApJ*, 473, L37  
 Halpern, J. P., & Wang, F. Y.-H. 1997, *ApJ*, 477, 905  
 Hermsen, W., et al. 1992, *IAU Circ.* 5541  
 Kuzmin, A. D., & Losovsky, B. Ya. 1997, *Astron. Lett.*, 23, 323  
 Malofeev, V., & Malov, I. F. 1997, *Nature*, 389, 697  
 Mattox, J. R., et al. 1992, *ApJ*, 401, L23  
 Mattox, J. R., et al. 1994, in *AIP Conf. Proc.* 304, *The Second Compton Symposium*, ed. C. Fichtel, N. Gehrels, & J. Norris (New York: AIP), 77  
 Mattox, J. R., Halpern, J. P., & Caraveo, P. A. 1996, *A&AS*, 120, C77  
 Mayer-Hasselwander, H., et al. 1994, *ApJ*, 421, 276  
 Michelson, P. F., 1996, *Proc. SPIE* 2806, *Gamma-Ray and Cosmic-Ray Detectors, Techniques, and Missions*, ed. B. D. Ramsey & T. A. Parnell (Bellingham, WA: SPIE), 31  
 Press, W. H., Teukolsky, S. A., Vetterling, W. T., & Flannery, B. P. 1992, *Numerical Recipes in C* (Cambridge: Cambridge Univ. Press)  
 Shabanova, T. 1995, *ApJ*, 453, 779  
 Shemar, S. L., & Lyne, A. G. 1996, *MNRAS*, 282, 677  
 Shitov, Yu. P., & Pugachev, V. D. 1997, *New Astron.*, submitted  
 Shklovskii, I. S. 1970, *Soviet Astron.*, 13, 562  
 Taylor, J. H., Manchester, R. N., & Lyne, A. G. 1993, *ApJS*, 88, 529  
 Thompson, D. J., et al. 1977, *ApJ*, 213, 252  
 Thorsett, S. E., Arzoumanian, Z., & Taylor, J. H. 1993, *ApJ*, 412, L33  
 Vats, H. O., Deshpande, M. R., Shah, C., Singal, A. K., Iyer, K. N., Oza, R., & Doshi, S. 1997, *IAU Circ.* 6699  
 Wang, F. Y.-H., Ruderman, M., Halpern, J. P., & Zhu, T. 1997, in preparation  
 Wolszczan, A. 1994, *Science*, 264, 538